

*Short note***Photoproduction of neutral pion pairs from the proton**

M. Wolf¹, J. Ahrens², R. Beck², V. Hejny¹, J.D. Kellie³, M. Kotulla¹, B. Krusche^{1,a}, V. Kuhr⁴, R. Leukel², V. Metag^{1,b}, J.C. Nacher⁶, R. Novotny¹, V. Olmos de León², R.O. Owens³, F. Rambo⁴, A. Schmidt², M. Schumacher⁴, U. Siodlaczek⁵, H. Ströher^{1,c}, J. Weiß¹, and F. Wissmann⁴

¹ II. Physikalisches Institut, Universität Gießen, D-35392 Gießen, Germany

² Institut für Kernphysik, Johannes-Gutenberg-Universität Mainz, D-55099 Mainz, Germany

³ Department of Physics and Astronomy, University of Glasgow, Glasgow G128QQ, UK

⁴ II. Physikalisches Institut, Universität Göttingen, D-37073 Göttingen, Germany

⁵ Physikalisches Institut, Universität Tübingen, D-72076 Tübingen, Germany

⁶ Departamento de Física Teórica and IFIC, Universidad de Valencia, 46100 Burjassot, Spain

Received: 6 June 2000 / Revised version: 27 July 2000

Communicated by Th. Walcher

Abstract. Double neutral pion photoproduction from the proton has been measured at MAMI for photon energies between threshold and 820 MeV. The reaction was identified by an invariant mass and missing mass analysis. From threshold up to 370 MeV the total cross-section does not exceed 30 nb. For higher energies it shows a smooth rise until it reaches a maximum of about 10 μb at $E_\gamma = 740$ MeV. Dalitz plots of $m^2(\pi^0, \pi^0)$ versus $m^2(p, \pi^0)$ for seven bins of incident photon energy have been analysed. For $E_\gamma > 610$ MeV, a strong contribution of a sequential decay is observed with the $\Delta(1232)$ -resonance as intermediate state. A comparison to model calculations shows that these sequential decays presumably originate from the $D_{13}(1520)$ - and also the $P_{11}(1440)$ -resonance.

PACS. 13.60.Le Meson production – 25.20.Lj Photoproduction reactions

1 Introduction

Nucleon resonances have been studied in a variety of experiments in an attempt to obtain information on the structure of the nucleon by comparison to quark-model calculations. With the advent of continuous wave electron accelerators during the last ten years, high-quality measurements have been performed using electromagnetic probes.

Although nucleon resonances overlap because of their large width, it is possible to study the properties of individual resonances by choosing selective decay channels: *e.g.*, the $\Delta(1232)$ can be examined by photoproduction of single π -mesons [1] while the η -meson is a selective probe of the $S_{11}(1535)$ -resonance [2]. The photoproduction of pion pairs is sensitive to the properties of the $P_{11}(1440)$ and $D_{13}(1520)$ -resonances. While the reaction channels with at least one charged pion are measured quite well

[3] only few data on the photoproduction of two neutral pions [4, 5] are available. This reaction provides interesting details because many Born terms are strongly suppressed and most nucleon resonances as well as the $\rho^0(770)$ cannot directly decay into two neutral pions.

Our measurement overcomes limitations of previously published data which were mainly limited in statistical accuracy. A comparison of the new data with different model calculations is of particular interest because the existing theoretical predictions [6–8] differ strongly from each other and cannot consistently describe the available experimental results for the different isospin channels.

2 Experimental setup

The experiment was performed at the Mainz accelerator facility MAMI [9] using the Glasgow-Mainz tagging spectrometer [10] and the Two-Arm Photon-Spectrometer TAPS [11].

The MAMI accelerator delivered a continuous beam of 880 MeV electrons. The energy of the bremsstrahlung photons was determined by measuring the energy difference between the incident and the scattered electron. The

^a *Present address:* Department of Physics and Astronomy, University of Basel, CH-4056 Basel, Switzerland.

^b e-mail: Volker.Metag@exp2.physik.uni-giessen.de

^c *Present address:* Institut für Kernphysik, Forschungszentrum Jülich GmbH, D-52425 Jülich, Germany.

latter was detected in the tagging spectrometer with an energy resolution of about 2 MeV for photons between 300 and 820 MeV. The average photon flux was 500 kHz/(2 MeV).

Mesons were produced in a liquid hydrogen target of cylindrical shape with a length of 10 cm and a diameter of 4 cm. The decay photons of the neutral pions were detected in TAPS. In this experiment, TAPS comprised 384 BaF₂ scintillation crystals and 120 BaF₂-plastic phoswich telescopes [12], covering 33% of 4 π . The BaF₂ detectors were arranged in six blocks in a matrix of 8 \times 8 detectors each. These blocks were mounted in a horizontal plane around the target at polar angles of ± 50 , ± 100 and ± 150 degrees respectively. All BaF₂ crystals were equipped with individual plastic scintillators identifying charged particles. The forward wall, consisting of 120 phoswich telescopes, had a hexagonal shape covering polar angles between 5 and 20 degrees with respect to the photon beam direction. Further details of the experimental setup are found in ref. [13].

3 Data analysis

The TAPS photon spectrometer provides several methods to separate photons from other particles. Besides charged particle vetoing, a pulse-shape analysis of the BaF₂ signals and rigid cuts on the time-of-flight of the decay photons can be applied. A detailed description of these procedures is, *e.g.*, given in ref. [4,14].

The objective of the analysis is to identify the reaction channel $\gamma p \rightarrow \pi^0 \pi^0 p$. For most aspects of the analysis only kinematically fully reconstructed events have been utilized, *i.e.* the 4-momenta of all particles are known. For events with at least four photons it is checked that they originate from the decay of two neutral pions. The pions are identified by their invariant mass using

$$m_{\gamma_1 \gamma_2} = \sqrt{2E_{\gamma_1} E_{\gamma_2} (1 - \cos \phi_{12})},$$

where E_{γ_1} and E_{γ_2} are the energies of two photons and ϕ_{12} is the opening angle between them. In a first step the invariant masses of all combinations of the detected photons are calculated. For four photons this leads to three pairs of invariant masses.

Events are further processed if both invariant masses equal that of a π^0 in at least one of the combinations. For incident photon energies below the η -production threshold of $E_\gamma = 707.9$ MeV this cut is sufficient to identify the reaction. Above this energy the analysis becomes more difficult. The η has a branching ratio of 32.2% into $3\pi^0$. Because of the limited acceptance of TAPS this decay can mimic a $2\pi^0$ event. In this energy regime the proper reaction channel is determined by a missing mass analysis which cleanly separates the two reactions.

Near the production threshold for $2\pi^0$ mesons, the cross-section is very small. Hence, the total cross-section

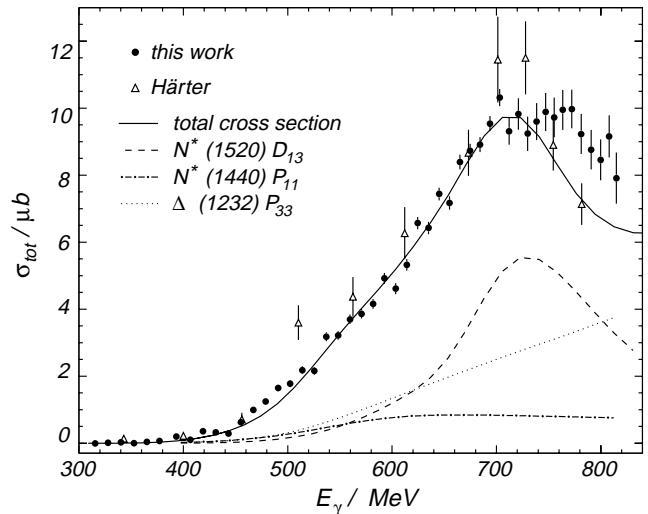


Fig. 1. Total cross-section of the $2\pi^0$ photoproduction from the proton as a function of the incident photon energy. The present result is compared to a previous measurement [4] and to a calculation with the model of ref. [6]. Within this model, the contributions of different baryon resonances are indicated.

for incident photon energies below 440 MeV was also extracted from events with only three coincident decay photons detected in TAPS (open symbols in fig. 2) one pair of which had an invariant mass equal to that of the π^0 . All these events were assigned to the $2\pi^0$ photoproduction process; as known from a recent measurement [15] a contamination from the $\gamma p \rightarrow p\pi^0\gamma'$ reaction amounts to less than 5 nb. In the given detector geometry, the detection efficiency for this reaction is lower by almost an order of magnitude near the $2\pi^0$ threshold.

Accidental coincidences between TAPS and the tagging spectrometer were eliminated by the subtraction of scaled distributions of random background events outside the true coincidence time window.

The incoming photon flux is derived from the scalers of the tagging spectrometer taking the regularly measured tagging efficiency into account.

The acceptance of TAPS and the analysis efficiency have been simulated with the GEANT3 program package [16] assuming phase space distributions for the particles in the final state. These simulations also take into account interactions in the target cell and the mechanical setup.

4 Results and discussion

4.1 Total cross-section

The total cross-section of the reaction $\gamma p \rightarrow \pi^0 \pi^0 p$ is shown in fig. 1 as a function of the incident photon energy in comparison to the previous measurement of ref. [4].

Three theoretical predictions have been published for this reaction [6–8]. The measured cross-section is best reproduced by the model of Gomez-Tejedor and Oset [6] apart from slight deviations at the highest incident photon energies. In this model the strongest reaction channel

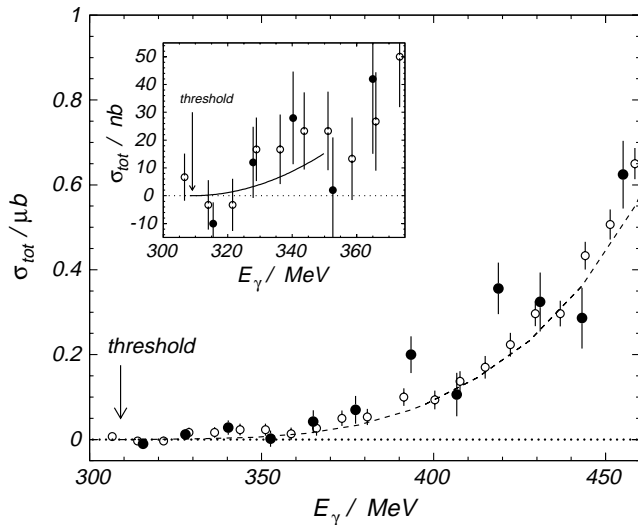


Fig. 2. Total cross-section of the reaction $\gamma p \rightarrow \pi^0 \pi^0 p$ close to the production threshold of 308.8 MeV. The solid and open circles are the result of an analysis with four and three detected photons per event, respectively. The dashed curve represents a calculation with the model of ref. [6]. The inset shows the measured total cross-section in comparison to a calculation based on chiral perturbation theory [8].

is the sequential decay of the $D_{13}(1520)$ -resonance via an intermediate $\Delta(1232)$ ($D_{13}(1520) \rightarrow \pi^0 \Delta \rightarrow \pi^0 \pi^0 p$).

The improved statistics of the present measurement allows the determination of the total cross-section near the production threshold at $E_\gamma = 308.8$ MeV (fig. 2). The cross-section starts at threshold with a very slow and smooth rise. A value of 30 nb is reached at an energy of 60 MeV above threshold. Below this energy, the data can be compared with calculations based on chiral perturbation theory. The prediction of Bernard *et al.* [8], shown in the inset of fig. 2, is in reasonable agreement with the present measurement.

4.2 Dalitz plots

For a more detailed investigation of the reaction mechanism, Dalitz plots have been analysed. In a standard representation, the number of events is plotted as a function of two squared invariant masses calculated from the three particles in the final state. If the momenta of the particles are distributed according to phase space the plot becomes a flat plateau while structures in the Dalitz plot indicate resonant intermediate states or particle correlations.

The relevant variables of the reaction $\gamma p \rightarrow \pi^0 \pi^0 p$ are $m^2(p, \pi_1^0)$, $m^2(p, \pi_2^0)$, and $m^2(\pi_1^0, \pi_2^0)$. Since the two pions are indistinguishable, all information can be extracted from a single Dalitz plot $m^2(p, \pi^0)$ versus $m^2(\pi_1^0, \pi_2^0)$ which has two entries per event. Figure 3 shows this Dalitz plot for different bins of incident photon energy. The plots for photon energies above 610 MeV exhibit a distinct deviation from a flat distribution which is much weaker in the two lowest bins.

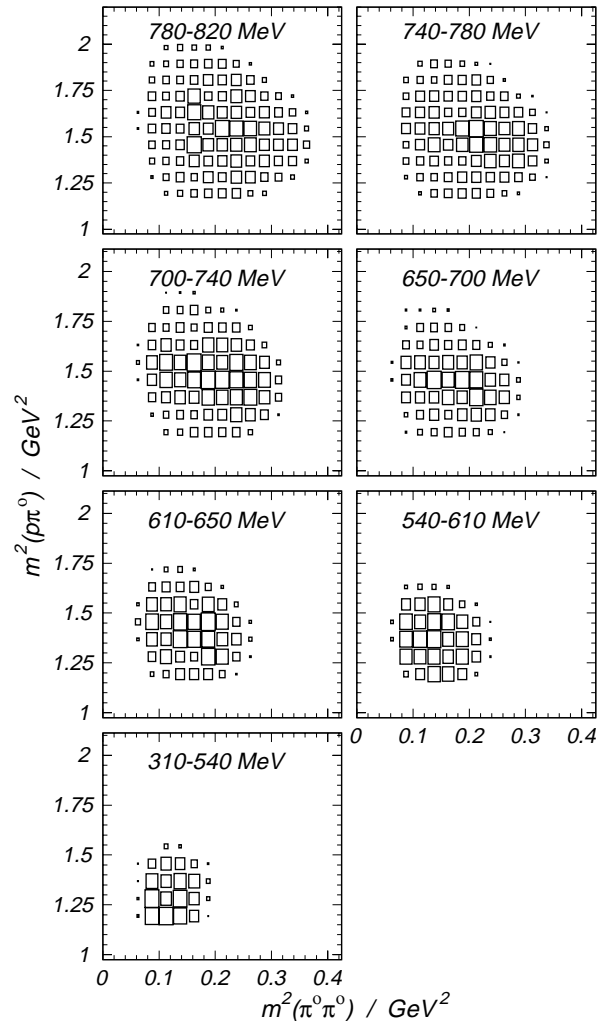


Fig. 3. Acceptance corrected Dalitz plots for the reaction $\gamma p \rightarrow \pi^0 \pi^0 p$ for different incident photon energy bins. The squared invariant mass of $\pi^0 \pi^0$ versus that of $\pi^0 p$ is shown. There are thus two entries per event. The size of the boxes scales linearly with the intensity.

Figure 4 shows the measured invariant masses of $m(\pi_1^0, \pi_2^0)$ together with the expected shape of a reaction without any intermediate resonant state (phase-space distribution). Below 740 MeV, the distributions predicted by the model of ref. [6] are in good agreement with the data although a phase-space distribution is consistent as well. In general, the data do not show a very strong correlation between the pions.

The invariant masses of proton and pion $m(p, \pi^0)$ for the same energy bins show a different behavior. While the two lowest measured distributions (310–540 MeV, 540–610 MeV) agree with phase space, the others do not. There is a significant enhancement at the mass of the Δ -resonance. This proves the population of an intermediate $\Delta^+(1232)$ -resonance. Note that there are two entries per event in these histograms corresponding to the two pions. If one of the pions originates from the decay of a Δ the other one cannot be correlated with the proton at all. Consequently,

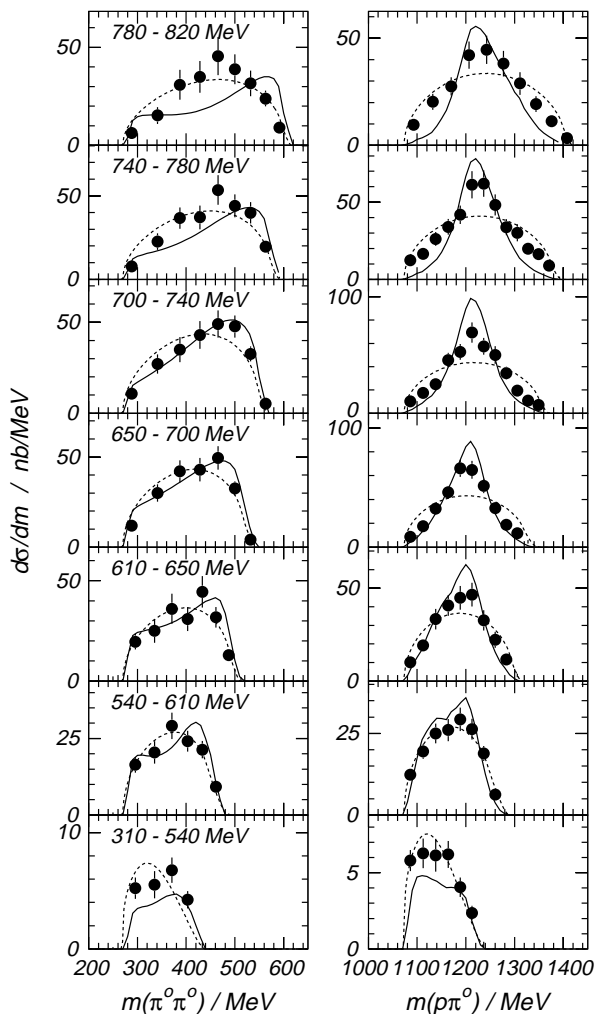


Fig. 4. Invariant mass of $\pi^0\pi^0$ (lhs) and π^0p (rhs) for different bins of incident photon energy. The dashed curves correspond to a reaction dominated by pure phase space. The solid curves are calculations with the model of ref. [6].

if one could pick the proper pion the signal would be even more distinct.

The deviation from phase space starts at incident photon energies between 610 and 650 MeV, *i.e.* just below the maximum of the $P_{11}(1440)$ -resonance and the point where the mechanism which involves the $D_{13}(1520)$ -resonance channel is opening. The most pronounced Δ signal appears already in the three following bins (650–780 MeV). This is precisely the region dominated by the $D_{13}(1520)$ excitation as shown in fig. 1. Hence, the large Δ peak in the $p\pi^0$ invariant mass spectra around these energies indicates a decay of the $D_{13}(1520)$ -resonance into the $\pi^0\Delta$ channel, leading to the $\pi^0\pi^0p$ final state. This is the dominant decay mode in the model of Gomez-Tejedor and Oset [6]. The sequential decay of the $P_{11}(1440)$ -resonance

[17] ($P_{11}(1440) \rightarrow \pi^0\Delta \rightarrow \pi^0\pi^0p$) also contributes but less than that of the $D_{13}(1520)$ -resonance.

5 Summary and conclusions

Photoproduction of two neutral pions from the proton has been measured for photon energies between threshold and 820 MeV. By detecting the four decay photons of the pions the reaction was identified unambiguously via an invariant mass and a missing mass analysis.

The very small total cross-section in the threshold region is in good agreement with the predictions of chiral perturbation theory [8] and the model of Gomez-Tejedor and Oset [6] is fairly consistent with the data over the whole energy range. In order to follow the evolution of different reaction mechanisms, Dalitz plots ($m^2(\pi^0, \pi^0)$ versus $m^2(p, \pi^0)$) for different incident photon energies have been analysed and compared to model calculations. The sequential decay of the $D_{13}(1520)$ -resonance via the $P_{33}(1232)$ -resonance is confirmed. A second weaker contribution could stem from the sequential decay of the $P_{11}(1440)$ -resonance. It will be interesting to compare these results with the data for the other isospin channels of two pion photoproduction.

We acknowledge the outstanding support of the accelerator group of MAMI, as well as many other scientists and technicians of the Institut für Kernphysik at the University of Mainz. This work was supported by the Deutsche Forschungsgemeinschaft (SFB 201) and the U.K. Engineering and Physical Sciences Research Council.

References

1. M. Fuchs et al., Phys. Lett. B **368**, 20 (1996), M. MacCormick et al. Phys. Rev. C **53**, 41 (1996).
2. B. Krusche et al., Phys. Rev. Lett. **74**, 3736 (1995).
3. A. Zabrodin et al., Phys. Rev. C **60**, 055201 (1999).
4. F. Härter et al., Phys. Lett. B **401**, 229 (1997).
5. A. Braghieri et al., Phys. Lett. B **363**, 46 (1995).
6. J. A. Gomez-Tejedor and E. Oset, Nucl. Phys. A **600**, 413 (1996).
7. K. Ochi and M. Hirata, Phys. Rev. C **56**, 1472 (1997).
8. V. Bernard et al., Phys. Lett. B **382**, 19 (1996).
9. Th. Walcher, Prog. Part. Nucl. Phys. **24**, 189 (1990).
10. I. Anthony et al., Nucl. Instrum. Meth. A **301**, 230 (1991).
11. R. Novotny, IEEE Trans. Nucl. Sci. **38**, 379 (1991).
12. R. Novotny, IEEE Trans. Nucl. Sci. **43**, 1260 (1996).
13. V. Hejny et al., Eur. Phys. J. A **6**, 83 (1999).
14. F. M. Marqués, Nucl. Instrum. Meth. A **365**, 392 (1995).
15. M. Kotulla, Univ. Giessen, private communication.
16. R. Brun et al., GEANT, Cern/DD/ee/84-1, 1986.
17. C. Caso et al., *Review of Particle Physics*, Eur. Phys. J. C **3**, 1 (1998).